O. J. P. Éboli[1*], M. C. Gonzalez-García[2], S. M. Lietti[1], and S. F. Novaes[1]
[1] *Instituto de Física Teórica, Universidade Estadual Paulista, Rua Pamplona 145, 01405–900, São Paulo, Brazil*
[2] *Instituto de Física Corpuscular IFIC CSIC, Universidad de Valencia, Edificio Institutos de Paterna, Apartado 2085, 46071 Valencia*

We analyze the potential of the Fermilab Tevatron and CERN Large Hadron Collider (LHC) to study anomalous quartic vector–boson interactions $\gamma\gamma ZZ$ and $\gamma\gamma W^+W^-$. Working in the framework of $SU(2)_L \otimes U(1)_Y$ chiral Lagrangians, we study the production of photons pairs accompanied by $\ell^+\ell^-$, $\ell^\pm\nu$, and jet pairs to impose bounds on these new couplings, taking into account the unitarity constraints. We compare our findings with the indirect limits coming from precision electroweak measurements as well as with presently available direct searches at LEPII. We show that the Tevatron Run II can provide limits on these quartic limits which are of the same order of magnitude as the existing bounds from LEPII searches. LHC will be able to tighten considerably the direct constraints on these possible new interactions, leading to more stringent limits than the presently available indirect ones.

I. INTRODUCTION AND FORMALISM

Within the framework of the Standard Model (SM), the structure of the trilinear and quartic vector boson couplings is completely determined by the $SU(2)_L \times U(1)_Y$ gauge symmetry. The study of these interactions can either lead to an additional confirmation of the model or give some hint on the existence of new phenomena at a higher scale [1]. Presently, the triple gauge–boson couplings are being probed at the Tevatron [2] and LEP [3] through the production of vector boson pairs, however, we have only started to study directly the quartic gauge–boson couplings [4,5].

It is important to independently measure the trilinear and quartic gauge boson couplings because there are extensions of the SM [6] that leave the trilinear couplings unchanged but do modify the quartic vertices. A simple way to generate, at tree level, new quartic gauge boson interactions is, for instance, by the exchange of a heavy boson between vector boson pairs.

The phenomenological studies of the anomalous vertices $\gamma\gamma W^+W^-$ and $\gamma\gamma ZZ$ have already been carried out for $\gamma\gamma$ [7,8], $e\gamma$ [9], and e^+e^- [10] colliders. Some preliminary estimates of the potential of the Tevatron collider have been also presented in Ref. [11] where only the effect on the total cross section for "neutral" final states γW^+W^- and $\gamma\gamma Z$ were considered while the most promising charged final state $\gamma\gamma W^\pm$ was not included. In this paper we analyze the potential of hadron colliders to unravel deviations on the quartic vector boson couplings by examining the most relevant processes which are the production of two photons accompanied by a lepton pair, where the fermions are produced by the decay of either a $W^\pm$ or a Z^0 in the anomalous contribution, *i.e.*

$$p + p\ (\bar{p}) \to \gamma + \gamma + (W^* \to)\ \ell + \nu\ , \tag{1}$$
$$p + p\ (\bar{p}) \to \gamma + \gamma + (Z^* \to)\ \ell + \ell\ , \tag{2}$$

as well as the production of photon pairs accompanied by jets

$$p + p \to \gamma + \gamma + j + j \tag{3}$$

for the LHC.

We carry out a detailed analysis of these reactions taking into account the full SM background leading to the same final state. We introduce realistic cuts in order to reduce this background and we include the effect of detector efficiencies in the evaluation of the attainable limits. We further consider the energy dependence (form factor) of the anomalous couplings in order to comply with the unitarity bounds. Our results show that although the analysis of Tevatron Run I data can only provide limits on these quartic couplings which are worse than the existing bounds from LEPII searches, the Tevatron Run II could yield bounds of the same order of magnitude as the present LEPII limits.

*Address after October 2000: Instituto de Física da USP, C.P. 66.318, São Paulo, SP 05389-970, Brazil.

Moreover, the LHC will be able to tighten considerably the direct constraints on these possible new interactions, giving rise to limits more stringent than the presently available indirect bounds.

In order to perform a model independent analysis, we use a chiral lagrangian to parametrize the anomalous $\gamma\gamma W^+W^-$ and $\gamma\gamma ZZ$ interactions [12]. Assuming that there is no Higgs boson in the low energy spectrum we employ a nonlinear representation of the spontaneously broken $SU(2)_L \otimes U(1)_Y$ gauge symmetry. To construct such lagrangian, it is useful to define the matrix–valued scalar field $\xi(x) = \exp(2iX_a\varphi^a(x)/v)$, where X_a are the broken generators and φ^a are the Nambu–Goldstone bosons of the global symmetry-breaking pattern $SU(2)_L \otimes U(1)_Y \to U(1)_{em}$. We denote the unbroken generator by Q and our conventions are such that $\mathrm{Tr}(X_aX_b) = \frac{1}{2}\delta_{ab}$ and $\mathrm{Tr}(X_aQ) = 0$.

The action of a transformation G of the gauge group $SU(2)_L \otimes U(1)_Y$ on ξ takes the form

$$\xi \to \xi' \quad \text{where} \quad G\xi = \xi' H^\dagger \ . \tag{4}$$

$H = \exp(iQu)$ is defined requiring that ξ' contains only the broken generators. In order to write the effective lagrangian for the gauge bosons, it is convenient to introduce the auxiliary quantity

$$\mathcal{D}_\mu(\xi) \equiv \xi^\dagger\partial_\mu\xi - i\xi^\dagger(gW^a_\mu T_a + g'B_\mu Y)\xi \ , \tag{5}$$

where T_a and Y are the generators of $SU(2)_L$ and $U(1)_Y$ respectively.

Now we can easily construct fields which have a simple transformation law under $SU(2)_L \otimes U(1)_Y$:

$$e\mathcal{A}_\mu \equiv \mathrm{Tr}[Q\mathcal{D}_\mu(\xi)] \qquad e\mathcal{A}_\mu \to e\mathcal{A}_\mu + \partial_\mu u \ , \tag{6}$$

$$\sqrt{g^2+g'^2}\,\mathcal{Z}_\mu \equiv \mathrm{Tr}[X_3\mathcal{D}_\mu(\xi)] \qquad \mathcal{Z}_\mu \to \mathcal{Z}_\mu \ , \tag{7}$$

$$g\mathcal{W}^\pm_\mu \equiv i\sqrt{2}\mathrm{Tr}[T_\mp\mathcal{D}_\mu(\xi)] \qquad \mathcal{W}^\pm_\mu \to e^{\pm iuQ}\,\mathcal{W}^\pm_\mu \ , \tag{8}$$

with the standard definition $T_\pm = T_1 \pm iT_2$. Notice that the fields $\mathcal{A}$, $\mathcal{Z}$, and $\mathcal{W}^\pm$ transform only electromagnetically under $SU(2)_L \otimes U(1)_Y$. Therefore, effective lagrangians must be invariant exclusively under the unbroken $U(1)_{em}$. Moreover, in the unitary gauge ($\xi = 1$) we have that $\mathcal{A} \to A$, $\mathcal{Z} \to Z$, and $\mathcal{W}^\pm \to W^\pm$.

Requiring C and P invariance, the lowest order effective interactions involving photons is

$$\begin{aligned}\mathcal{L}_{\text{eff}} = &-\frac{\pi\alpha\,\beta_1}{2}\,F^{\mu\nu}F_{\mu\nu}\mathcal{W}^{+\alpha}\mathcal{W}^-_\alpha - \frac{\pi\alpha\,\beta_2}{4}\,F^{\mu\nu}F_{\mu\nu}\mathcal{Z}^\alpha\mathcal{Z}_\alpha \\ &-\frac{\pi\alpha\,\beta_3}{4}\,F^{\mu\alpha}F_{\mu\beta}(\mathcal{W}^+_\alpha\mathcal{W}^{-\beta} + \mathcal{W}^+_\beta\mathcal{W}^{-\alpha}) - \frac{\pi\alpha\,\beta_4}{4}\,F^{\mu\alpha}F_{\mu\beta}\mathcal{Z}_\alpha\mathcal{Z}^\beta \ .\end{aligned} \tag{9}$$

In order to avoid the strong low energy constraints coming from the ρ parameter we impose the custodial $SU(2)$ symmetry which leads to $\beta_1 = c^2_W\beta_2 = \beta_0$ and $\beta_3 = c^2_W\beta_4 = \beta_c$. With this choice $\mathcal{L}_{eff}$ reduces to the parametrization used in Ref. [7]. In the unitary gauge, (9) gives rise to anomalous $\gamma\gamma ZZ$ and $\gamma\gamma W^+W^-$ vertices which are related by the custodial symmetry.

II. PRESENT CONSTRAINTS: PRECISION DATA, LEPII, AND UNITARITY BOUNDS

The couplings defined in the effective lagrangian (9) contribute at the one–loop level to the Z physics [9] via oblique corrections as they modify the W, Z, and photon two–point functions, and consequently they can be constrained by precision electroweak data. We denote the new contribution to the two–point functions as $\Pi_{VV(0,c)}$ and we take here the opportunity to update the constraints on β_0 and β_c derived in Ref. [9].

It is easy to notice from the structure of the lagrangians that the contributions to the W and Z self–energies are constant, *i.e.* they do not depend on the external momentum. Moreover, due to the $SU(2)$ custodial symmetry they are related by

$$\Pi_{WW(0,c)} = c^2_w\Pi_{ZZ(0,c)} \ . \tag{10}$$

As a consequence the couplings β_0 and β_c do not contribute to $T = \Delta\rho$ [13]. Equivalently their contribution to $\sin\overline{\theta_W}$ vanishes. Moreover, the unbroken $U(1)_{em}$ symmetry constrains the photon self-energy contribution to be of the form

$$\Pi_{\gamma\gamma(0,c)}(q^2) = q^2\Pi'_{\gamma\gamma(0,c)} \ , \tag{11}$$

where for the anomalous interactions (9) $\Pi'_{\gamma\gamma(0,c)}$ is a constant. This also implies that these anomalous interactions do not modify the running of the electromagnetic coupling. However, both interactions give rise to corrections to Δr or, equivalently, to the S and U parameters [13].

Following the standard procedure, we evaluated the vector boson two–point functions using dimensional regularization and subsequently kept only the leading non–analytic contributions from the loop diagrams to constrain the new interactions — that is, we maintained only the logarithmic terms, dropping all others. The contributions that are relevant for our analysis are easily obtained by the substitution

$$\frac{2}{4-d} \to \log \frac{\Lambda^2}{\mu^2} \; ,$$

where Λ is the energy scale which characterizes the appearance of new physics, and μ is the scale in the process, which we take to be M_W. After this procedure we obtain that

$$\begin{aligned} \alpha S &= -4 s_W^2 c_W^2 \Pi'_{\gamma\gamma} \\ &= -4 s_W^2 c_W^2 \left\{ \frac{\alpha\, \beta_0 M_W^2}{4\pi} \left[-\left(1 + \frac{1}{2c_W^4}\right) + \frac{3}{2} \ln\left(\frac{\Lambda^2}{M_W^2}\right) + \frac{3}{4c_W^4} \ln\left(\frac{\Lambda^2 c_W^2}{M_W^2}\right) \right] \right. \\ &\quad \left. + \frac{\alpha\, \beta_c M_W^2}{64\pi} \left[-\left(1 + \frac{1}{2c_W^4}\right) + 6 \ln\left(\frac{\Lambda^2}{M_W^2}\right) + \frac{3}{c_W^4} \ln\left(\frac{\Lambda^2 c_W^2}{M_W^2}\right) \right] . \right\} \; , \end{aligned} \tag{12}$$

$$\alpha U = \frac{s_w^2}{c_W^2} S \; . \tag{13}$$

The allowed ranges of S and U depend on the SM parameters. As an illustration of the size of the bounds, we take that for the Higgs boson mass of $M_H = 300$ GeV, the 95%CL limits on S and U are $0.34 \leq S \leq 0.02$ and $-0.13 \leq U \leq 0.37$ [14]. These bounds can then be translated into the 95% CL limits on β_0 and β_c presented in Table I.

The LEP collaborations have directly probed anomalous quartic couplings involving photons. L3 and OPAL have searched for their effects in the reactions $e^+e^- \to W^+W^-\gamma$, $Z\gamma\gamma$, and $\nu\bar{\nu}\gamma\gamma$, while the ALEPH collaboration has reported results only on the last reaction [4,5]. The combined results for all these searches lead to the following 95% CL direct limits on the quartic vertices [5]

$$-4.9 \times 10^{-3}\ \text{GeV}^{-2} \ < \ \beta_0 \ < \ 5.6 \times 10^{-3}\ \text{GeV}^{-2} \; , \tag{14}$$

$$-5.4 \times 10^{-3}\ \text{GeV}^{-2} \ < \ \beta_c \ < \ 9.8 \times 10^{-3}\ \text{GeV}^{-2} \; . \tag{15}$$

Another way to constrain the couplings in (9) is to notice that this effective lagrangian leads to tree-level unitarity violation in $2 \to 2$ processes at high energies. In order to extract the unitarity bounds on the anomalous interactions we evaluated the partial wave helicity amplitudes ($\tilde{a}^j_{\nu\mu}$) for the inelastic scattering $\gamma(\lambda_1)\gamma(\lambda_2) \to V(\lambda_3)V(\lambda_4)$, with $V = Z$ and $W^\pm$; see Table II. Unitarity requires that [15]

$$\beta_V \sum_\nu |\tilde{a}^j_{\nu\mu}|^2 \leq \frac{1}{4} \; , \tag{16}$$

where β_V is the velocity of the final state boson in the center–of–mass frame. For the anomalous interactions (9), the most restrictive bounds come from the $J = 0$ partial wave, which read

$$\left(\frac{\alpha\beta s}{16}\right)^2 \left(1 - \frac{4M_W^2}{s}\right)^{1/2} \left(3 - \frac{s}{M_W^2} + \frac{s^2}{4M_W^4}\right) \leq N \text{ for } V = W \; , \tag{17}$$

$$\left(\frac{\alpha\beta s}{16c_W^2}\right)^2 \left(1 - \frac{4M_Z^2}{s}\right)^{1/2} \left(3 - \frac{s}{M_Z^2} + \frac{s^2}{4M_Z^4}\right) \leq N \text{ for } V = Z \; , \tag{18}$$

where $\beta = \beta_0$ or β_c and $N = 1/4$ (4) for β_0 (β_c). For instance, unitarity is violated for $\gamma\gamma$ invariant masses above 240 GeV for $\beta_0 = 5.6 \times 10^{-3}$ GeV^{-2} (one of the present LEP bounds).

These unitarity constraints are of relevance when extracting the bounds on the anomalous couplings at hadron colliders since it is possible to obtain large parton–parton center–of–mass energies, and consequently have a large unitarity violation. The standard procedure to avoid this unphysical behavior of the subprocess cross section and to obtain meaningful limits is to multiply the anomalous couplings by a form factor

$$\beta_{0,c} \longrightarrow \left(1 + \frac{M_{\gamma\gamma}^2}{\Lambda^2}\right)^{-n} \times \beta_{0,c} \; , \tag{19}$$

where $M_{\gamma\gamma}$ is the invariant mass of the photon pair. Of course using this procedure the limits become dependent on the exponent n and the scale Λ which is not longer factorizable. In our calculations, we conservatively choose $n = 5$ and $\Lambda = 0.5$ TeV for the Tevatron and $\Lambda = 0.5$ (2.5) TeV for the LHC. In the case of e^+e^- colliders the center–of–mass energy is fixed and the introduction of the form factor (19) is basically equivalent to a rescaling of the anomalous couplings $\beta_{0,c}$, therefore we should perform this rescaling when comparing results obtained at hadron and e^+e^- colliders. For example, for our choice of n and Λ the LEP limits should be weakened by a factor $\simeq 1.6$.

The dynamical effect of the above form factor can be seen in Figure 1 where we present the normalized invariant mass distribution of the $\gamma\gamma$ pair for the process (1) at the Tevatron Run II and LHC, assuming that only β_0 contributes. As expected, the form factor reduces the number of photon pairs with high invariant mass. Similar behavior is obtained for reaction (2) and for the anomalous β_c contribution.

III. SIGNALS AT HADRON COLLIDERS

In this work we studied the reactions (1) and (2) for the Tevatron and LHC, that is, the associated production of a photon pair and a W^* or Z^* which decay leptonically, as well as the process (3) only for the LHC since the Tevatron center–of–mass energy is too low for this process to be of any significance. Process (1) can be used to study the $\gamma\gamma W^+W^-$ vertex while process (2) probes the $\gamma\gamma ZZ$ interaction and the reaction (3) receives contributions from $\gamma\gamma W^+W^-$ and $\gamma\gamma ZZ$. We evaluated numerically the helicity amplitudes of all the SM subprocesses leading to the $\gamma\gamma\ell^\pm\nu$, $\gamma\gamma\ell^+\ell^-$, and $\gamma\gamma jj$ final states where j can be either a gluon, a quark or an antiquark. The SM amplitudes were generated using Madgraph [16] in the framework of Helas [17] routines. The anomalous interactions arising from the Lagrangian (9) were implemented as subroutines and were included accordingly. We consistently took into account the effect of all interferences between the anomalous and the SM amplitudes, and did not use the narrow–width approximation for the vector boson propagators.

In the case of the Tevatron collider, we considered the parameters of the Run I, *i.e.* $\sqrt{s} = 1.8$ TeV and an integrated luminosity of 100 pb^{-1}. We also investigated the reach of the Tevatron Run II assuming $\sqrt{s} = 2$ TeV and an integrated luminosity of 2×10^3 pb^{-1}. For the LHC, we took a center–of–mass energy of 14 TeV and a luminosity of 10^5 pb^{-1}. In our calculations we used the MRS (G) [18] set of proton structure functions with the factorization scale $Q^2 = \hat{s}$.

We started our analysis of the processes (1) and (2) imposing a minimal set of cuts to guarantee that the photons and charged leptons are detected and isolated from each other:

$$\begin{aligned} p_T^{(\ell,\nu)} &\geq 20 \ \ (25) \text{ GeV for } \ell = e \ \ (\mu) \,, \\ E_T^\gamma &\geq 20 \text{ GeV} \ \ , \\ |\eta_{\gamma,e}| &\leq 2.5 \,, \\ |\eta_\mu| &\leq 1.0 \,, \\ \Delta R_{ij} &\geq 0.4 \,, \end{aligned} \tag{20}$$

where i and j stand for the final photons and charged leptons. For the $\gamma\gamma\ell\nu$ final state, we also imposed a cut the transverse mass of the $\ell\nu$ pair ($M_T^{\ell\nu}$)

$$65 \text{ GeV} \ \leq M_T^{\ell\nu} \leq 100 \text{ GeV} \ \ . \tag{21}$$

In the case of $\gamma\gamma\ell^+\ell^-$ production, we required the tag of a Z decaying leptonically imposing that

$$75 \text{ GeV} \ \leq M^{\ell\ell} \leq 105 \text{ GeV} \,, \tag{22}$$

where $M^{\ell\ell}$ is the invariant mass of the lepton pair. In our calculations, we have also taken into account the detection efficiency of the final state particles. We assumed a 85% detection efficiency of isolated photons, electrons, and muons. Therefore, the efficiency for reconstructing the final state $\gamma\gamma\ell\nu$ is 61% while the efficiency for $\gamma\gamma\ell^+\ell^-$ is 52%.

Considering the cuts (20), (21), and (22), and the detection efficiencies discussed above, the SM prediction for the cross sections and expected number of events of the processes (1) and (2) are presented in Table III. As we can see, the above basic cuts are enough to eliminate the SM background at the Tevatron Run I, however, further cuts are needed to control the background at the Tevatron Run II and LHC.

In order to reduce the SM background for the Tevatron Run II and LHC, we analyzed a few kinematical distributions. The most significant difference between the SM and anomalous predictions appears in the transverse energy of the photons, which is shown in Figure 2 for the reaction (1) and $\beta_0 \neq 0$. Similar behavior is obtained for the reaction (2) and for the anomalous β_c contribution. Therefore, we tightened the cut on the transverse energy of the final photons, as suggested by Fig. 2, to enhance the significance of the anomalous contribution.

$$E_T^{\gamma_{1(2)}} \geq 75 \ \ (50) \text{ GeV for Tevatron Run II and} \qquad (23)$$
$$E_T^{\gamma_{1(2)}} \geq 200 \ \ (100) \text{ GeV for LHC .}$$

The effect of these cuts can be seen in Table III where we display the new cross sections and expected number of events in parenthesis. As we can see, no SM event is expected at the Tevatron Run II after this new cut, while very few events survive at the LHC.

We parametrized the cross sections for processes (1) and (2) after cuts (20)–(23) as

$$\sigma \equiv \sigma_{\rm sm} + \beta\ \sigma_{\rm inter} + \beta^2\ \sigma_{\rm ano}\ , \qquad (24)$$

where $\sigma_{\rm sm}$, $\sigma_{\rm inter}$, and $\sigma_{\rm ano}$ are, respectively, the SM cross section, interference between the SM and the anomalous contribution and the pure anomalous cross section. β stands for β_0 or β_c. The results for $\sigma_{\rm sm}$, $\sigma_{\rm inter}$, and $\sigma_{\rm ano}$ are presented in Table IV.

Process (3) receives contributions from W^* and Z^* productions and their subsequent decay into jets, as well as from vector boson fusion (VBF)

$$p + p \to q + q + (W^* + W^* \text{ or } Z^* + Z^*) \to q + q + \gamma + \gamma\ . \qquad (25)$$

The signal for hadronic decays of W's and Z's is immersed in a huge QCD background. Therefore, we tuned our cuts in order to extract the VBF production of photon pairs since it presents two very energetic forward jets that can be used to efficiently tag the events. In our analyses, we required that the photons satisfy

$$\begin{aligned} E_T^{\gamma_{1(2)}} &> 50\ (25) \text{ GeV}\ , \\ |\eta_{\gamma_{(1,2)}}| &< 5.0\ , \end{aligned} \qquad (26)$$

while the jets should comply with

$$\begin{aligned} p_T^{j_{1(2)}} &> 40\ (20) \text{ GeV}\ , \\ |\eta_{j_{(1,2)}}| &< 5.0\ , \\ |\eta_{j_1} - \eta_{j_2}| &> 4.4\ , \\ \eta_{j_1}.\eta_{j_2} &< 0\ \ , \\ \min\{\eta_{j_1}, \eta_{j_1}\} + 0.7 < \eta_{\gamma_{(1,2)}} &< \max\{\eta_{j_1}, \eta_{j_1}\} - 0.7\ , \\ \Delta R_{jj} &> 0.7\ , \\ \Delta R_{j\gamma} &> 0.7\ . \end{aligned} \qquad (27)$$

Assuming a 85% detection efficiency of isolated photons, the efficiency for reconstructing the final state $jet+jet+\gamma+\gamma$ is 72%. Table III also contains the SM cross section for the VBF production of photon pair taking into account the above cuts. As we can see, the VBF reaction possesses a much higher statistics than the production of photon pairs associated to leptons. In order to enhance the VBF signal for the anomalous couplings we studied a few kinematical distributions and found out that the most significant difference between the signal and SM background occurs in the diphoton invariant mass spectrum; see Fig. 3. Thusly, we imposed the following additional cuts

$$200\ (400) \text{ GeV}\ \leq M_{\gamma\gamma} \leq 700\ (2500) \text{ GeV for } \Lambda = 500\ (2500) \text{ GeV}. \qquad (28)$$

This cut reduces the SM background cross section by a factor of at least 5; see Table III where we also present the signal cross section after cuts for $\Lambda = 500$ and 2500 GeV. The results for $\sigma_{\rm sm}$ and $\sigma_{\rm ano}$ of Eq. (24) are presented in Table IV. Since the interference between the SM and the anomalous contribution is negligible in this case, we do not present the results for $\sigma_{\rm inter}$.

Taking into account the integrated luminosities of the Tevatron and LHC and the results shown in Table IV, we evaluated the potential 95% CL limits on β_0 and β_c in the case that there is no deviation from the SM predictions; see Table V. We also exhibit in this table our choice for the scale Λ appearing in the form factor. Therefore, at the Tevatron, the most restrictive constraints are obtained from the reaction (1) for β_0 and β_c. Combining both reactions we are able to impose a 95% CL limit $|\beta_{0,c}| \lesssim 1.5 \times 10^{-2}$ GeV^{-2} at the Tevatron Run II, which is of the same order of the direct bounds coming from LEPII. On the other hand, the most stringent limits at the LHC will come from the photon pair production via VBF, whose bounds are a factor of 5–10 stronger than the ones coming from the reactions (1) and (2). This general statement does not seem to apply for the limits on β_c with $\Lambda = 500$ GeV, which is more strongly constrained by the process (1). This is not surprising because, for the reactions (1) and (2), the set of cuts (23) leave the β_c signal practically unaffected, i.e. this set of general cuts is particularly optimum for this coupling and reactions. This is also there reason why the derived limits on β_c are better than the limits for β_0 only for this case.

IV. SUMMARY AND CONCLUSIONS

We are just beginning to test the SM predictions for the quartic vector boson interactions. Due to the limited available center–of–mass energy, the first couplings to be studied contain two photons, and just at the LHC and the NLC we will be able to probe $VVVV$ ($V = W$ or Z) vertices [19]. In this work we analyzed the production of photon pairs in association with $\ell^{\pm}\nu$, $\ell^{+}\ell^{-}$, or jj in hadron colliders. These processes violate unitarity at high energy, therefore, we cutoff the growth of the subprocess cross section via the introduction of form factors which enforce unitarity and render the calculation meaningful.

We showed that the study of the processes (1) and (2) at Tevatron Run I lead to constraints on the quartic anomalous couplings that are a factor of four weaker than the presently available bounds derived from LEPII data. On the other hand, the Tevatron Run II has the potential to probe the quartic anomalous interactions at the same level of LEPII. An important improvement on the bounds on the genuine quartic couplings will be obtained at the LHC collider where, for $\Lambda = 2.5$ TeV, a limit of $|\beta_{0,c}| \lesssim 10^{-5}$ GeV^{-2} will be reached. Therefore, the direct limits on the anomalous interaction steaming from LHC will be stronger than the ones coming from the precise measurements at the Z pole. It is interesting to notice that the LHC will lead to limits that are similar to the ones attainable at an $e^{+}e^{-}$ collider operating at $\sqrt{s} = 500$ GeV with a luminosity of 300 pb^{-1}, which are $|\beta_{0,c}| \lesssim 3 \times 10^{-5}$ GeV^{-2} [10].

In conclusion, the LHC will be able to impose quite important limits on genuine quartic couplings studying the $\gamma\gamma\ell^{+}\ell^{-}$, $\gamma\gamma\ell\nu$, and $\gamma\gamma jj$ productions.

ACKNOWLEDGMENTS

This work was supported by Conselho Nacional de Desenvolvimento Científico e Tecnológico (CNPq), by Fundação de Amparo à Pesquisa do Estado de São Paulo (FAPESP), by Programa de Apoio a Núcleos de Excelência (PRONEX), by the spanish DGICYT under grants PB98-0693 and PB97-1261, by the Generalitat Valenciana under grant GV99-3-1-01, and by the TMR network grant ERBFMRXCT960090 of the European Union.

---

[1] For a review see: H. Aihara *et al.*, *Anomalous gauge boson interactions* in Electroweak Symmetry Breaking and New Physics at the TeV Scale, edited by T. Barklow, S. Dawson, H. Haber and J. Seigrist, (World Scientific, Singapore, 1996), p. 488 [hep-ph/9503425].

[2] K. Gounder, CDF Collaboration, hep-ex/9903038; B. Abbott *et al.*, DØ Collaboration, Phys. Rev. **D62**, 052005 (2000).

[3] R. Barate *et al.*, ALEPH Collaboration, Phys. Lett. **B462**, 389 (1999); P. Abreu *et al.*, DELPHI Collaboration, Phys. Lett. **B459**, 382 (1999); M. Acciarri *et al.*, L3 Collaboration, Phys. Lett. **B467**, 171 (1999); G. Abbiendi *et al.*, OPAL Collaboration, Eur. Phys. J. **C8**, 191 (1999).

[4] G. Abbiendi *et al.*, OPAL Collaboration, Phys. Lett. **B471**, 293 (1999); M. Acciarri *et al.*, L3 Collaboration, Phys. Lett. **B478**, 39 (2000); and hep-ex/0008022.

[5] S. Spagnolo, talk at the XXXth International Conference on High Energy Physics, Osaka July 2000, http://ichep2000.hep.sci.osaka-u.ac.jp/scan/0727/pa05/spagnolo/.

[6] A. Hill and J. J. van der Bij, Phys. Rev. D**36**, 3463 (1987); R. Casalbuoni, *et al.*, Nucl. Phys. **B282**, 235 (1987); *idem* Phys. Lett. **B155**, 95 (1985); S. Godfrey, *Quartic Gauge Boson Couplings* in Proceedings of the International Symposium on Vector Boson Self-Interactions, edited by U. Baur, S. Errede, T. Muller (American Inst. Phys., 1996), p. 209 [hep-ph/9505252].

[7] G. Bélanger and F. Boudjema, Phys. Lett. **B288**, 210 (1992).

[8] O. J. P. Éboli, M. B. Magro, P. G. Mercadante, and S. F. Novaes, Phys. Rev. **D52**, 15 (1995).

[9] O. J. P. Éboli, M. C. Gonzalez-Garcia, and S. F. Novaes, Nucl. Phys. **B411**, 381 (1994).

[10] G. Bélanger and F. Boudjema, Phys. Lett. **B288**,201 (1992); W. J. Stirling and A. Werthenbach, Phys. Lett. **B466**, 369 (1999); W. J. Stirling and A. Werthenbach, Eur. Phys. J. **C14**, 103 (2000); G. Belanger, F. Boudjema, Y. Kurihara, D. Perret-Gallix, and A. Semenov Eur. Phys. J. **C13**, 283 (2000).

[11] P. J. Dervan, A. Signer, W. J. Stirling, and A. Werthenbach , J. Phys. **G26**, 607 (2000).

[12] C. P. Burgess and D. London, Phys. Rev. **D48**, 4337 (1993).

[13] M. E. Peskin and T. Takeuchi, Phys. Rev. Lett. **65**, 964 (1990); Phys. Rev. D**46**, 381 (1992).

[14] D. E. Groom, *et al.*, Particle Data Group, Eur. Phys. J. **C15**, 1 (2000).

[15] U. Baur and D. Zeppenfeld, Nucl. Phys. **B308**, 127 (1988).

[16] T. Stelzer and W. F. Long, Comput. Phys. Commun. **81**, 357 (1994).

[17] H. Murayama, I. Watanabe, and K. Hagiwara, KEK report 91-11 (unpublished).
[18] A. D. Martin, W. J. Stirling, and R. G. Roberts, Phys. Lett. **B354**, 155 (1995).
[19] O. J. P. Éboli, M. C. Gonzalez–Garcia, and J. K. Mizukoshi, Phys. Rev. **D58**, 034008 (1998); T. Han, H.-J. He, and C.-P. Yuan, Phys. Lett. **B422**, 294 (1998); V. Barger, K. Cheung, T. Han, and R. J. N. Philips, Phys. Rev. **D52**, 3815 (1995); E. E. Boos, H. J. He , W. Kilian, A. Pukhov, and P. M. Zerwas, Phys. Rev. **D57**, 1553 (1997); J. Bagger, S. Dawson, and G. Valencia, Nucl. Phys. **B399**, 364 (1993); A. Dobado, D. Espriu, and M. J. Herrero, Z. Phys. **C50**, 205 (1991); A. S. Belyaev, *et al.*, Phys. Rev. **D59**, 015022 (1999); A. Dobado and M. T. Urdiales, Z. Phys. **C17**, 965 (1996); J. R. Pelaez, Phys. Rev. **D55**, 4193 (1997).

Λ (TeV)	Parameter	β_0 (GeV^{-2})	β_c (GeV^{-2})
0.5	S	$(\ -0.09\ ,\ 1.5\ )\times10^{-4}$	$(\ -0.29\ ,\ 4.9\ )\times10^{-4}$
	U	$(\ -5.4\ ,\ 1.9\ )\times10^{-4}$	$(\ -18.\ ,\ 6.2\ )\times10^{-4}$
2.5	S	$(\ -0.04\ ,\ 0.69\ )\times10^{-4}$	$(\ -0.15\ ,\ 2.5\ )\times10^{-4}$
	U	$(\ -2.5\ ,\ 0.88\ )\times10^{-4}$	$(\ -9.1\ ,\ 3.2)\times10^{-4}$

TABLE I. 95% CL limits on β_o and β_c steaming from oblique parameters S and U.

$(\lambda_1,\lambda_2,\lambda_3,\lambda_4)$	$\tilde{a}^0_{\nu\mu}$
$(++++)$ or $(--++)$	$\left(\frac{\alpha s}{16 n_V}\right)\beta$
$(++--)$ or $(----)$	$\left(\frac{\alpha s}{16 n_V}\right)\beta$
$(++00)$ or $(--00)$	$\left(1-\frac{s}{2M_V^2}\right)\left(\frac{\alpha s}{16 n_V}\right)\beta$

TABLE II. $\tilde{a}^0_{\nu\mu}$ for the reactions $\gamma(\lambda_1)\gamma(\lambda_2)\to V(\lambda_3)V(\lambda_4)$, with $V=Z$ and $W^\pm$, where $\mu=\lambda_1-\lambda_2$ and $\nu=\lambda_3-\lambda_4$. β stands for β_0 or β_c and $n_{W^\pm}=1$ (4) for β_0 (β_c) and $n_Z=c_W^2$ ($4c_W^2$) for β_0 (β_c).

Collider	Process	Cross Section (pb)	Number of Events
Tevatron I	$p\bar{p}\to l^\pm\nu_{l\pm}\gamma\gamma$	$1.93\ \times10^{-4}$	1.93×10^{-2}
	$p\bar{p}\to l^+l^-\gamma\gamma$	$1.58\ \times10^{-4}$	1.58×10^{-2}
Tevatron II	$p\bar{p}\to l^\pm\nu_{l\pm}\gamma\gamma$	$2.13\ \times10^{-4}$ $(7.89\ \times10^{-6})$	0.43 $(1.58\ \times10^{-2})$
	$p\bar{p}\to l^+l^-\gamma\gamma$	$1.77\ \times10^{-4}$ $(5.90\ \times10^{-6})$	0.35 $(1.18\ \times10^{-2})$
LHC	$pp\to l^\pm\nu_{l\pm}\gamma\gamma$	$1.08\ \times10^{-3}$ $(1.32\ \times10^{-5})$	108 (1.3)
	$pp\to l^+l^-\gamma\gamma$	$6.45\ \times10^{-4}$ $(4.25\ \times10^{-6})$	65 (0.43)
	$pp\to jj\gamma\gamma$	3.19×10^{-2} (6.28×10^{-3}) $[1.12\times10^{3}]$	3190 (628) [112]

TABLE III. SM cross sections after the cuts. We applied the cuts (20)–(22) to the $\ell\nu\gamma\gamma$ and $\ell^+\ell^-\gamma\gamma$ processes while we used the cuts (20) and (26,27) to the $\gamma\gamma jj$ final state. We present between parenthesis the Tevatron II results after we included the additional cut (23) for $\ell\nu\gamma\gamma$ and $\ell^+\ell^-\gamma\gamma$ productions. In the case of $jj\gamma\gamma$ production at LHC, we exhibit between parenthesis (brackets) the results after cuts (28) for $\Lambda=0.5$ (2.5) TeV.

Collider	Process	$\sigma_{\rm sm}$ (pb)	$\sigma_{\rm inter}$ (pb $\times$ GeV^2) for β_0 (β_c)	$\sigma_{\rm ano}$ (pb $\times$ GeV^4) for β_0 (β_c)
Tevatron I	$p\bar{p}\to l^\pm\nu_{l\pm}\gamma\gamma$	$1.93\ \times10^{-4}$	$5.09(2.58)\times10^{-3}$	15.0(5.50)
Λ=0.5 TeV	$p\bar{p}\to l^+l^-\gamma\gamma$	$1.58\ \times10^{-4}$	$7.18(1.22)\times10^{-3}$	3.63(1.37)
Tevatron II	$p\bar{p}\to l^\pm\nu_{l\pm}\gamma\gamma$	$7.89\ \times10^{-6}$	$1.20(1.03)\times10^{-3}$	6.21(2.92)
Λ=0.5 TeV	$p\bar{p}\to l^+l^-\gamma\gamma$	$5.90\ \times10^{-6}$	$1.38(0.36)\times10^{-3}$	1.78(0.86)
LHC	$pp\to l^\pm\nu_{l\pm}\gamma\gamma$	1.32×10^{-5}	$3.13(3.97)\times10^{-4}$	6.79(59.2)
Λ=0.5 TeV	$pp\to l^+l^-\gamma\gamma$	4.25×10^{-6}	$6.06(0.49)\times10^{-4}$	4.82(18.5)
	$pp\to jj\gamma\gamma$	6.28×10^{-3}	—	1.02×10^{4} (7.56×10^{2})
LHC	$pp\to l^\pm\nu_{l\pm}\gamma\gamma$	1.32×10^{-5}	$1.17(22.4)\times10^{-3}$	5570(2900)
Λ=2.5 TeV	$pp\to l^+l^-\gamma\gamma$	4.25×10^{-6}	$1.15(1.08)\times10^{-2}$	3980(1390)
	$pp\to jj\gamma\gamma$	1.12×10^{-3}	—	1.07×10^{7} (7.34×10^{5})

TABLE IV. Results for $\sigma_{\rm sm}$, $\sigma_{\rm inter}$ and $\sigma_{\rm ano}$; see Eq. (24). $\sigma_{\rm inter}$ and $\sigma_{\rm ano}$ are obtained for the anomalous coupling β_0 (β_c) in units of GeV^{-2}. We considered $n=5$ and different values of Λ; see Eq. (19).

Collider	Process	β_0 (GeV^{-2})	β_c (GeV^{-2})
Tevatron I	$p\bar{p} \to l^{\pm}\nu_{l^{\pm}}\gamma\gamma$	$(\ -4.5\ ,\ 4.4\ )\times 10^{-2}$	$(\ -7.4\ ,\ 7.4\ )\times 10^{-2}$
	$p\bar{p} \to l^{+}l^{-}\gamma\gamma$	$(\ -9.2\ ,\ 9.0\ )\times 10^{-2}$	$(\ -15.\ ,\ 15.\ )\times 10^{-2}$
Λ=0.5 TeV	Combined	$(\ -4.0\ ,\ 4.0\ )\times 10^{-2}$	$(\ -6.6\ ,\ 6.5\ )\times 10^{-2}$
Tevatron II	$p\bar{p} \to l^{\pm}\nu_{l^{\pm}}\gamma\gamma$	$(\ -1.6\ ,\ 1.5\ )\times 10^{-2}$	$(\ -2.3\ ,\ 2.2\ )\times 10^{-2}$
	$p\bar{p} \to l^{+}l^{-}\gamma\gamma$	$(\ -2.9\ ,\ 2.9\ )\times 10^{-2}$	$(\ -4.2\ ,\ 4.1\ )\times 10^{-2}$
Λ=0.5 TeV	Combined	$(\ -1.4\ ,\ 1.3\ )\times 10^{-2}$	$(\ -2.0\ ,\ 2.0\ )\times 10^{-2}$
LHC	$pp \to l^{\pm}\nu_{l^{\pm}}\gamma\gamma$	$(\ -2.2\ ,\ 2.1\ )\times 10^{-3}$	$(\ -7.4\ ,\ 7.3\ )\times 10^{-4}$
	$pp \to l^{+}l^{-}\gamma\gamma$	$(\ -2.4\ ,\ 2.3\ )\times 10^{-3}$	$(\ -12.\ ,\ 12.\ )\times 10^{-4}$
Λ=0.5 TeV	$pp \to jj\gamma\gamma$	$(\ -2.2\ ,\ 2.2)\times 10^{-4}$	$(\ -8.0\ ,\ 8.0\ )\times 10^{-4}$
LHC	$pp \to l^{\pm}\nu_{l^{\pm}}\gamma\gamma$	$(\ -7.6\ ,\ 7.6\ )\times 10^{-5}$	$(\ -11.\ ,\ 10.\ )\times 10^{-5}$
	$pp \to l^{+}l^{-}\gamma\gamma$	$(\ -8.2\ ,\ 7.9\ )\times 10^{-5}$	$(\ -14.\ ,\ 13.\ )\times 10^{-5}$
Λ=2.5 TeV	$pp \to jj\gamma\gamma$	$(\ -4.4\ ,\ 4.4\ )\times 10^{-6}$	$(\ -1.7\ ,\ 1.7\ )\times 10^{-5}$

TABLE V. 95% CL limits on β_0 and β_c that can be obtained at the Tevatron and LHC assuming that no deviation from the SM predictions is observed. We considered $n = 5$ and different values of Λ; see Eq. (19).

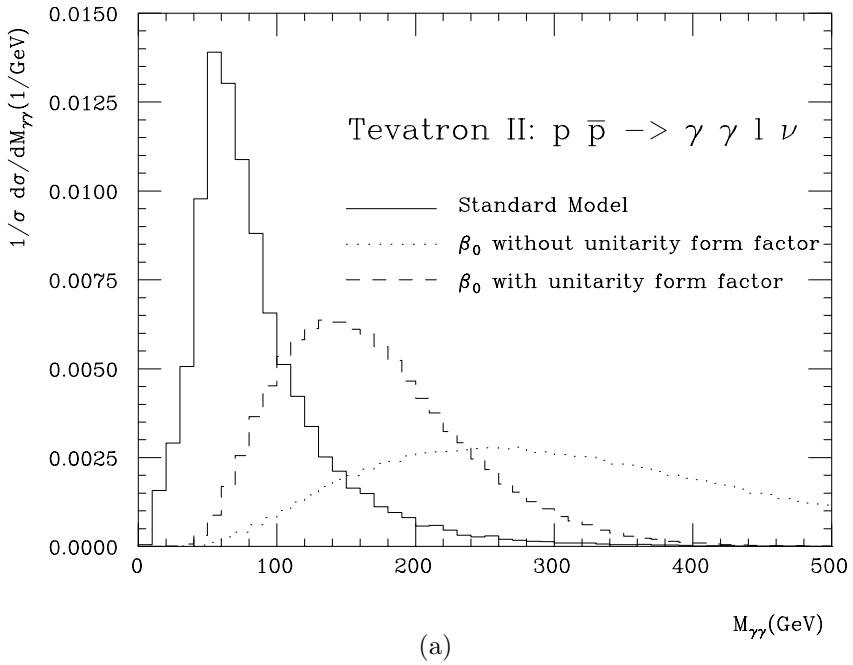

(a)

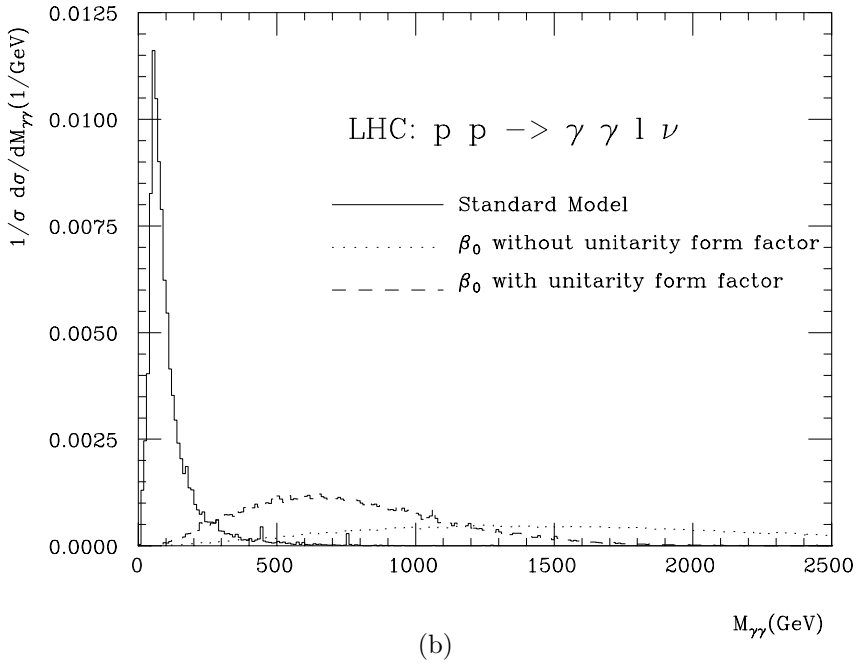

(b)

FIG. 1. Normalized invariant mass distribution of the $\gamma\gamma$ pair for the reaction $p+p\ (\bar{p}) \to \gamma+\gamma+(W^* \to)\ \ell+\nu$ at Tevatron Run II (a) and LHC (b). The solid histogram represents the SM contribution while dashed (dotted) histograms is the anomalous β_0 contribution with (without) unitarity form factor. We chose $n = 5$ and $\Lambda = 0.5$ (2.5) TeV for the Tevatron (LHC).

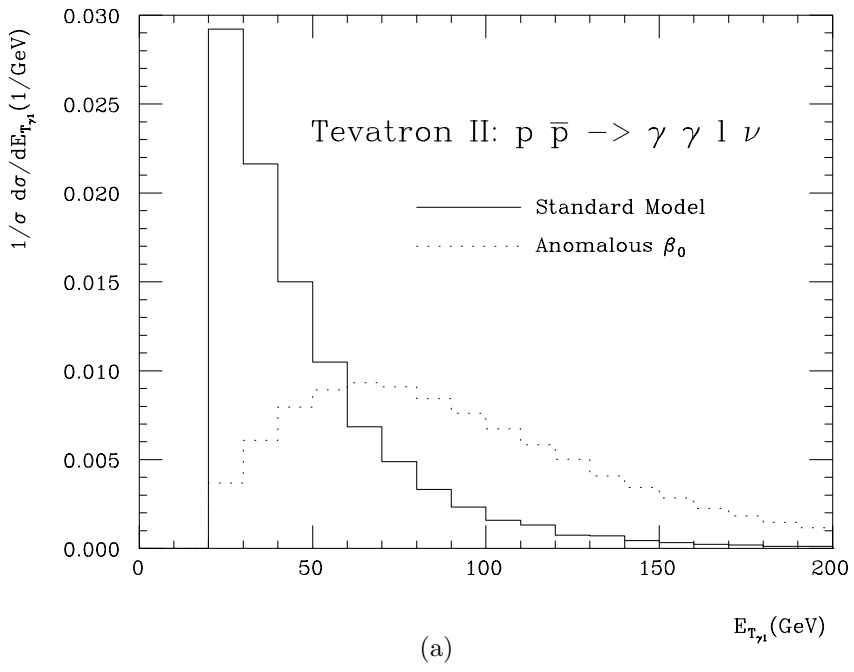

(a)

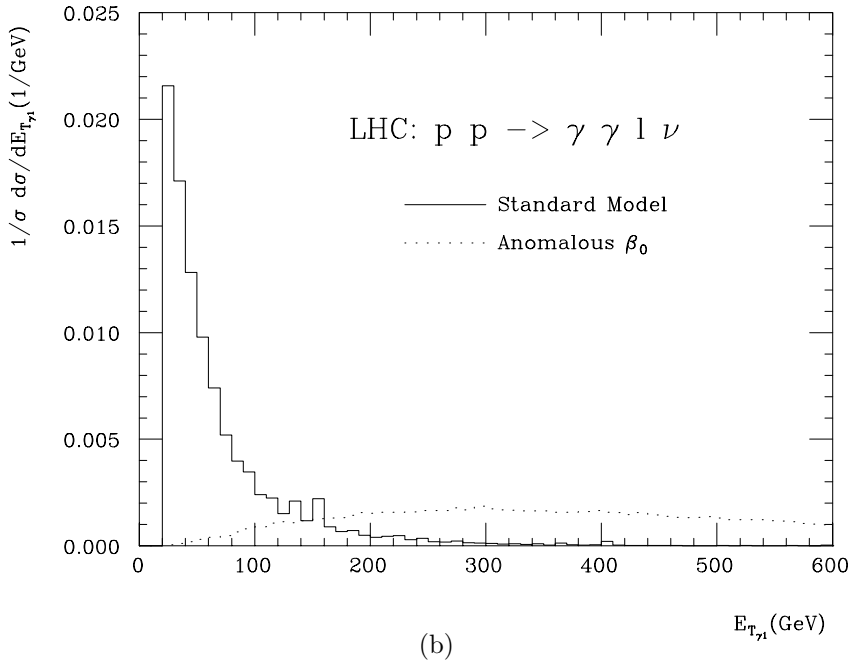

(b)

FIG. 2. Normalized transverse energy distribution of the most energetic photon for the reaction (1) at Tevatron Run II (a) and LHC (b). The solid histogram represents the SM contribution while the dotted one is the anomalous β_0 contribution.

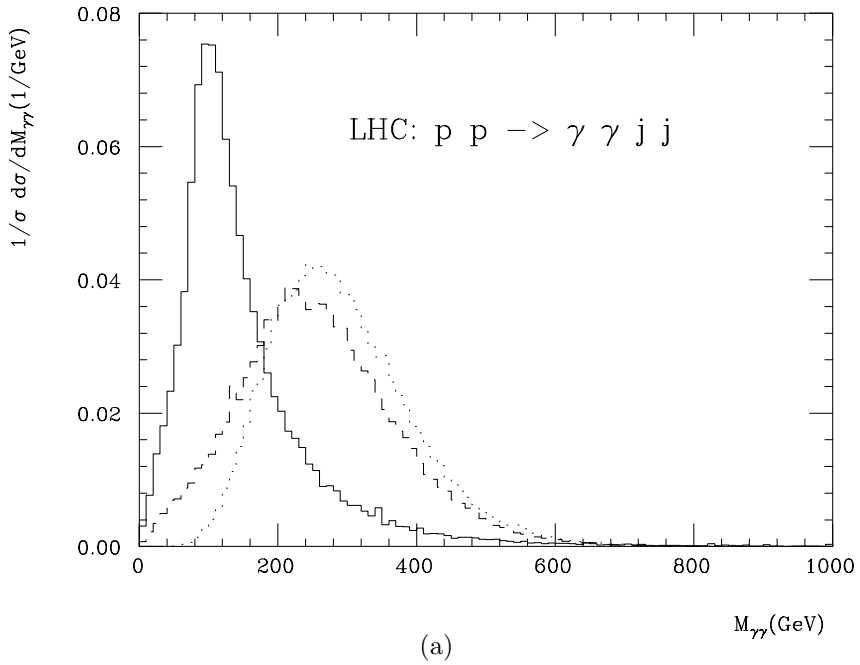

(a)

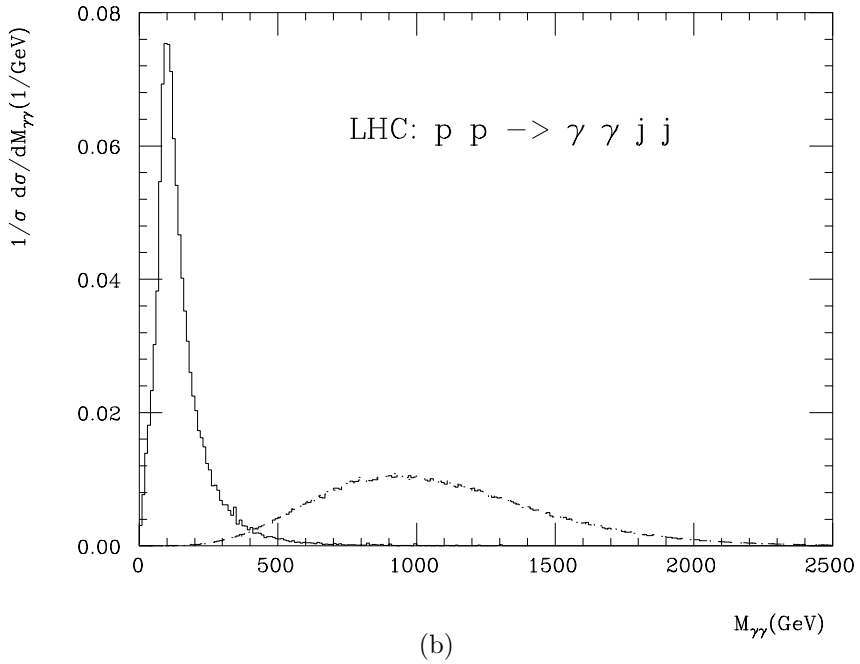

(b)

FIG. 3. Normalized invariant mass distribution of the $\gamma\gamma$ pair for the reaction $p + p \to \gamma + \gamma + jet + jet$ at LHC. The solid histogram represents the SM contribution while dotted (dashed) histograms is the anomalous β_0 (β_c) contribution with unitarity form factor. We chose $n = 5$ and (a) $\Lambda = 0.5$ TeV and (b) $\Lambda = 2.5$ TeV.

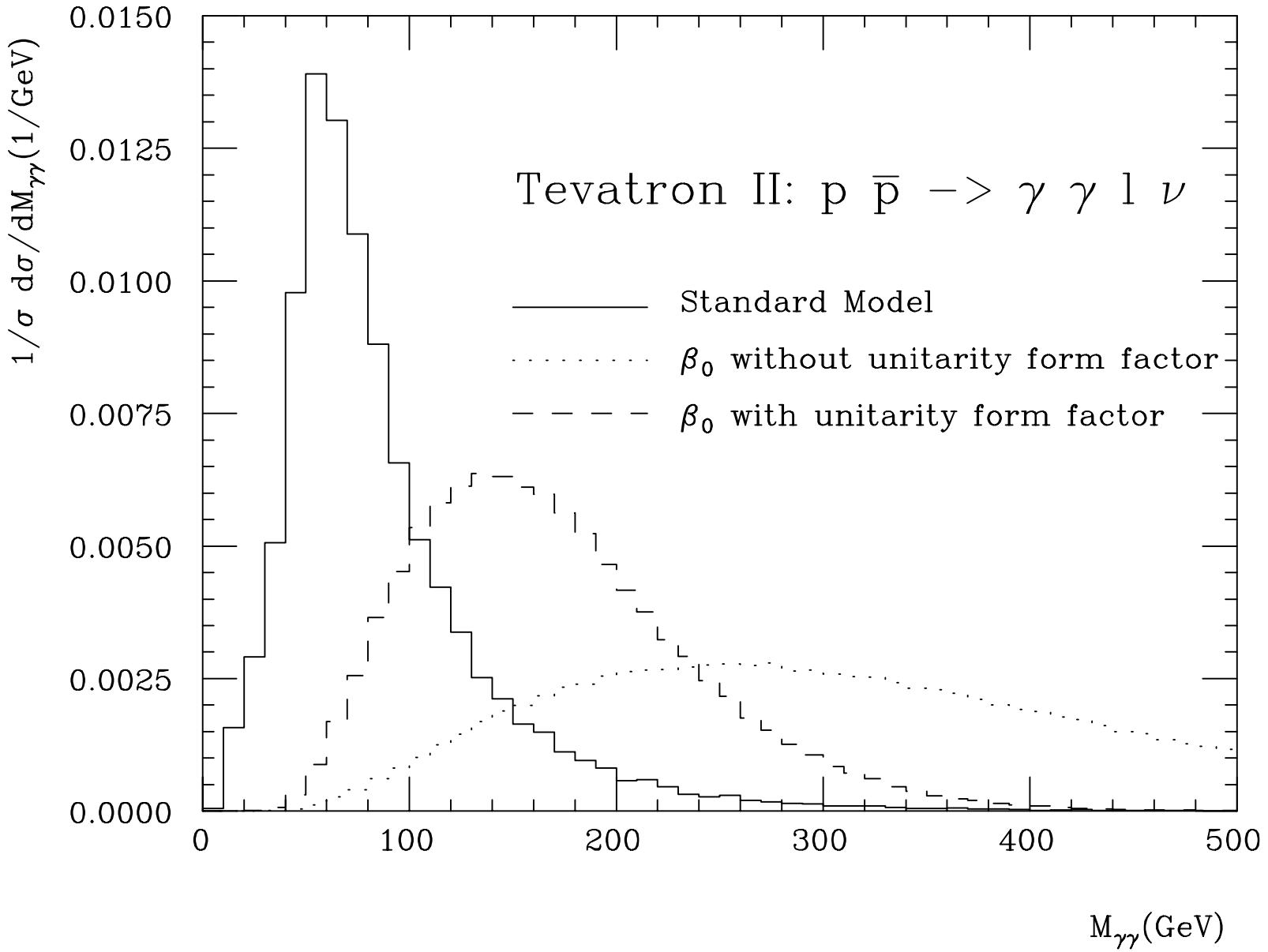
Tevatron II: p $\bar{p}$ -> γ γ l ν
Standard Model
β_0 without unitarity form factor
β_0 with unitarity form factor
1/σ dσ/dM$_{\gamma\gamma}$(1/GeV)
M$_{\gamma\gamma}$(GeV)
0.0150
0.0125
0.0100
0.0075
0.0050
0.0025
0.0000
0
100
200
300
400
500

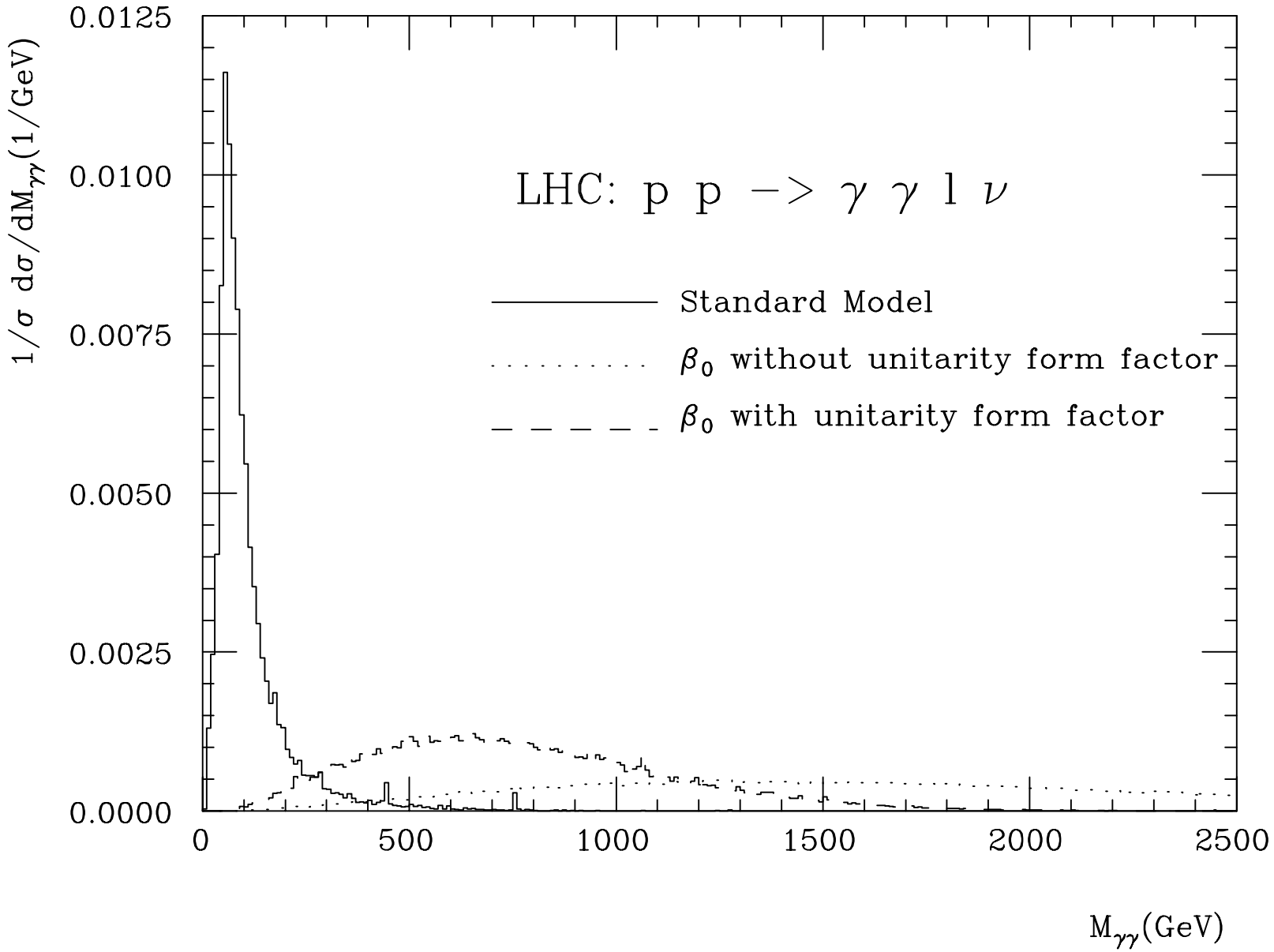
LHC: p p -> γ γ l ν
Standard Model
β0 without unitarity form factor
β0 with unitarity form factor
1/σ dσ/dMγγ(1/GeV)
Mγγ(GeV)
0.0125
0.0100
0.0075
0.0050
0.0025
0.0000
0
500
1000
1500
2000
2500

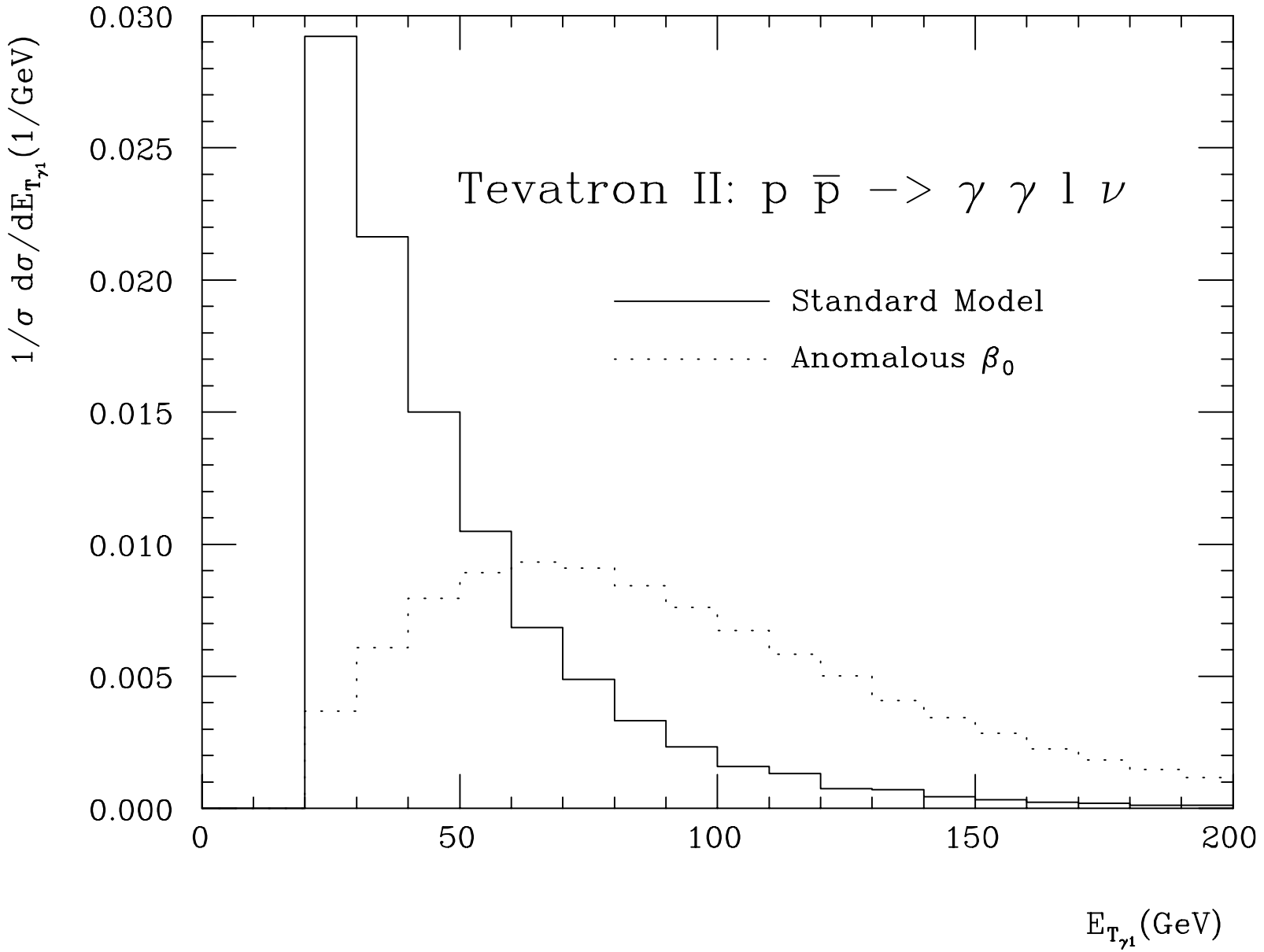
Tevatron II: p $\bar{p}$ -> γ γ l ν
Standard Model
Anomalous β_0
$1/\sigma\ d\sigma/dE_{T_{\gamma 1}}(1/GeV)$
$E_{T_{\gamma 1}}(GeV)$
0.030
0.025
0.020
0.015
0.010
0.005
0.000
0
50
100
150
200

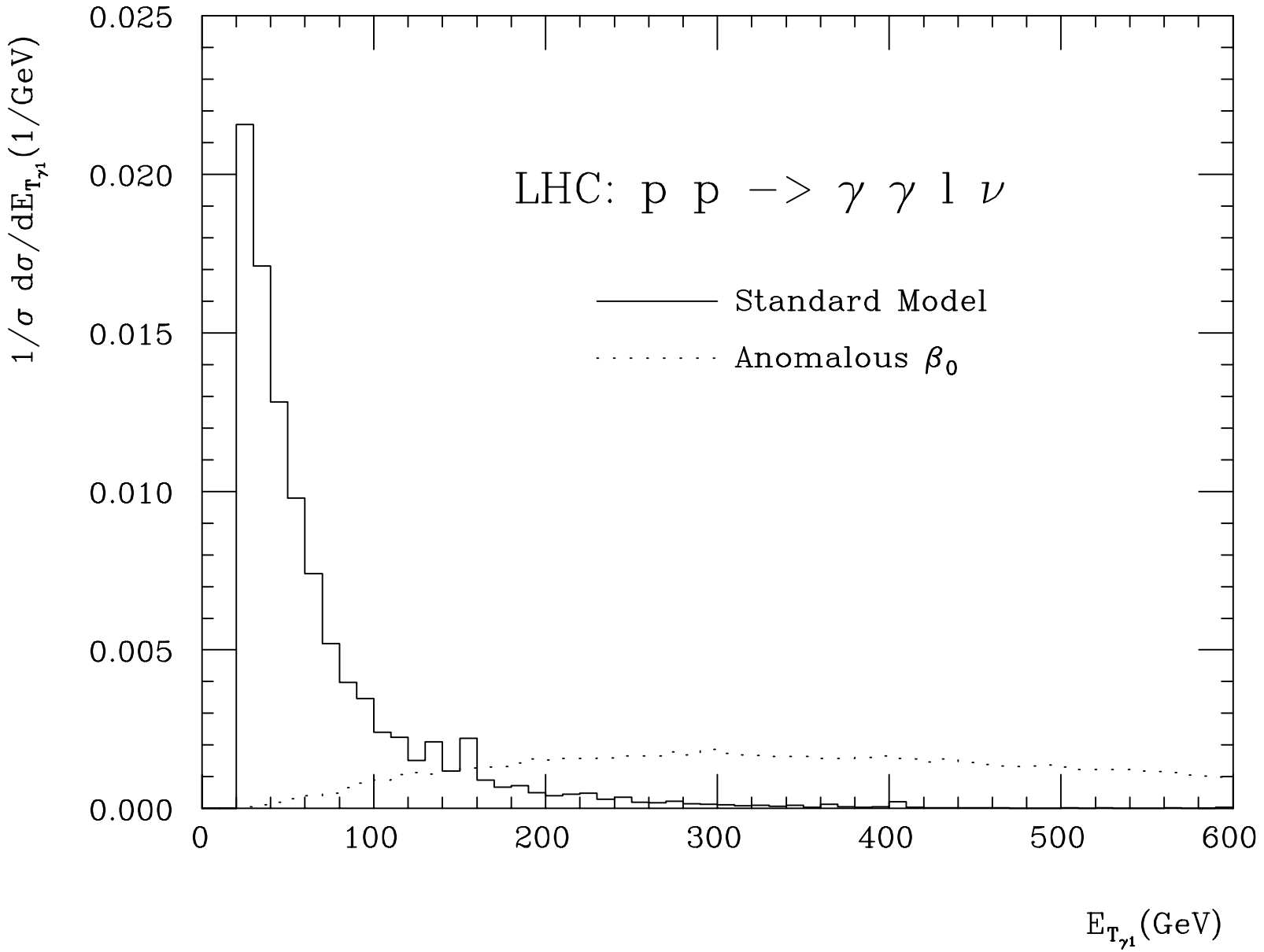
LHC: p p -> γ γ l ν
Standard Model
Anomalous β0
1/σ dσ/dE_Tγ1 (1/GeV)
E_Tγ1 (GeV)
0.025
0.020
0.015
0.010
0.005
0.000
0
100
200
300
400
500
600

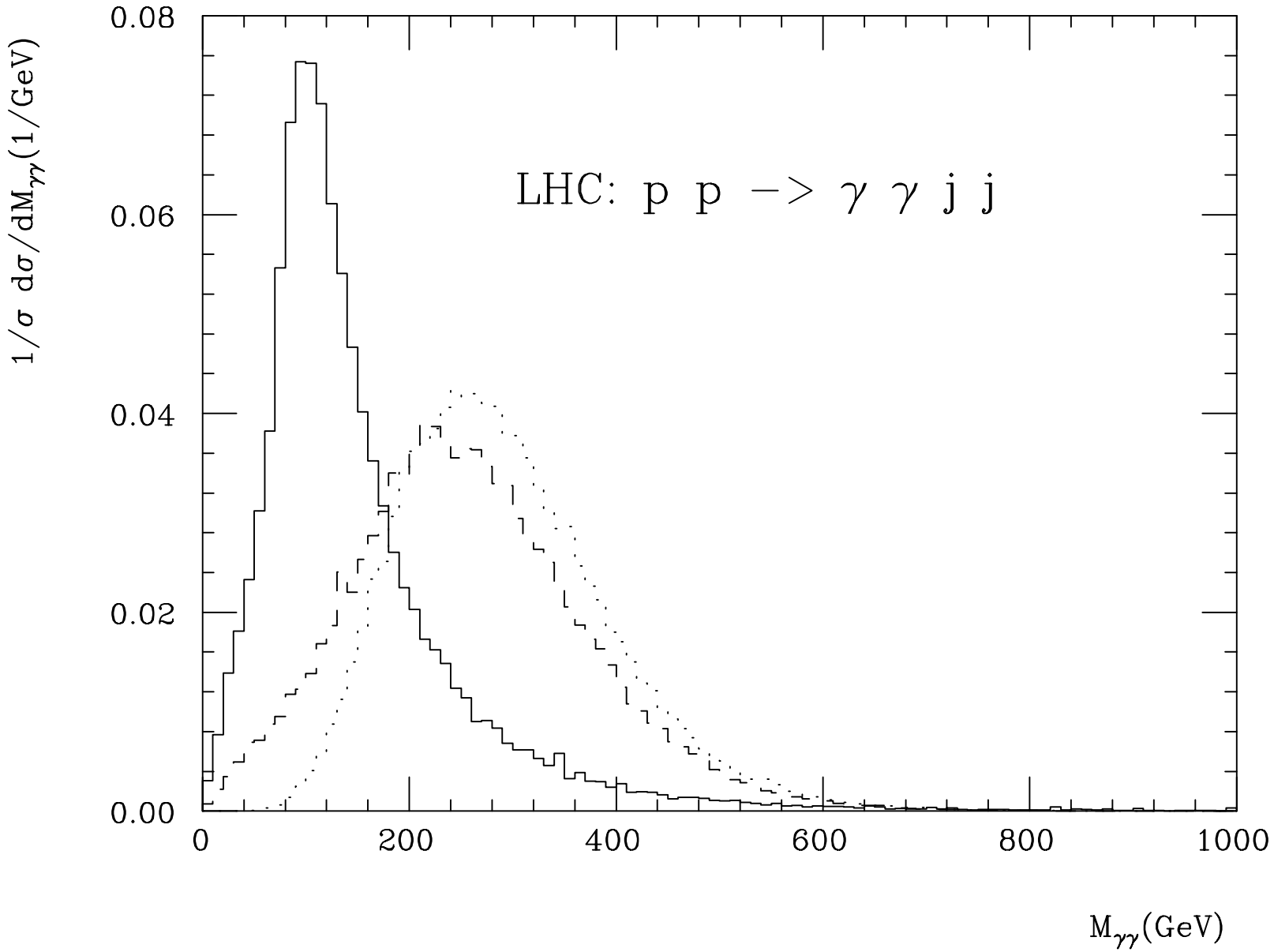
LHC: p p -> γ γ j j
1/σ dσ/dM$_{γγ}$(1/GeV)
M$_{γγ}$(GeV)
0.08
0.06
0.04
0.02
0.00
0
200
400
600
800
1000

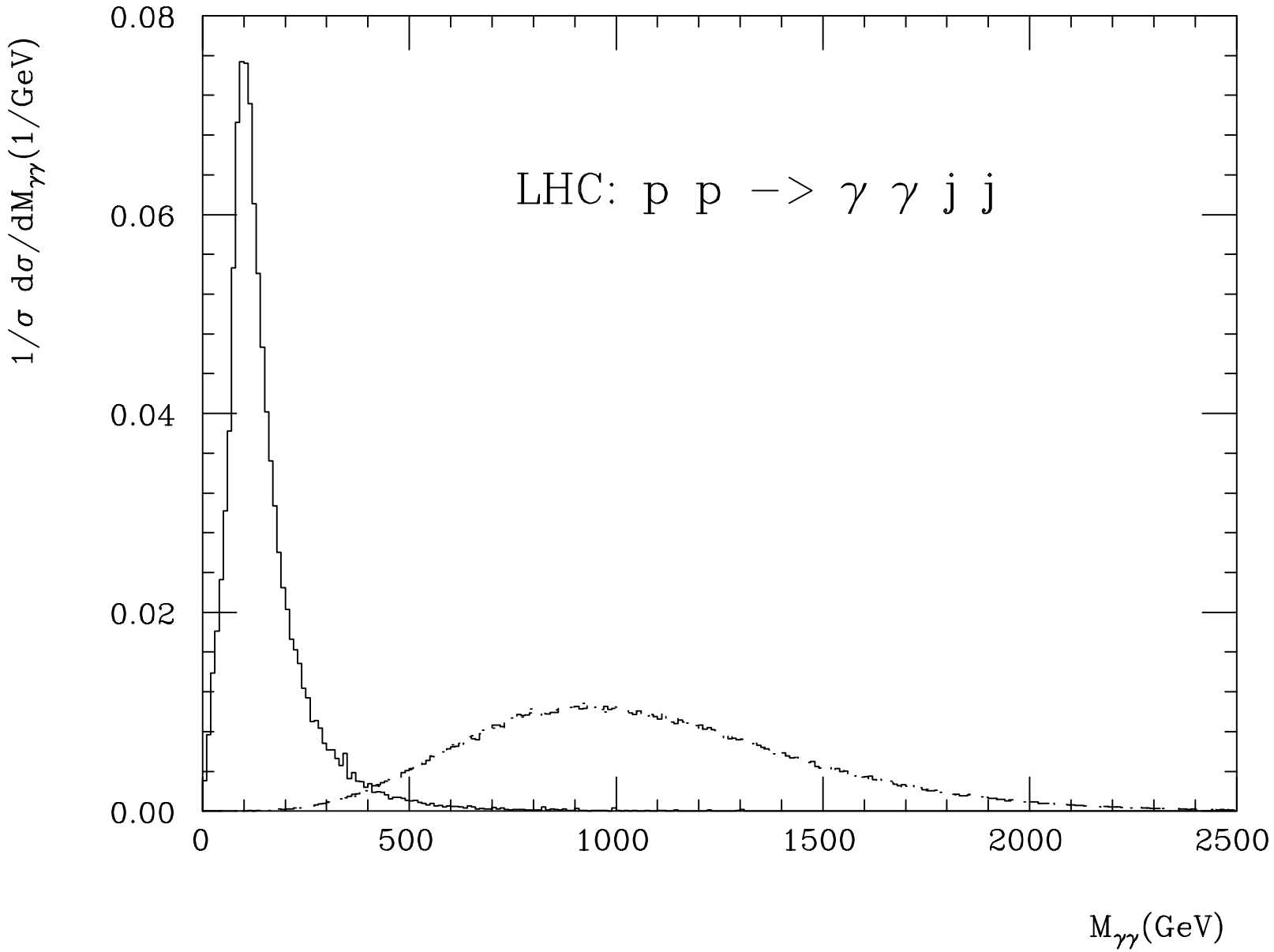
LHC: p p -> γ γ j j
1/σ dσ/dM$_{\gamma\gamma}$(1/GeV)
M$_{\gamma\gamma}$(GeV)
0.00
0.02
0.04
0.06
0.08
0
500
1000
1500
2000
2500